

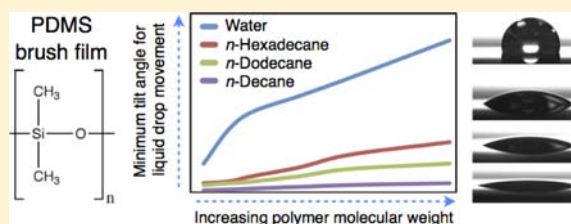
A Physical Approach To Specifically Improve the Mobility of Alkane Liquid Drops

Dalton F. Cheng, Chihiro Urata, Benjamin Masheder, and Atsushi Hozumi*

National Institute of Advanced Industrial Science and Technology, 2266-98, Anagahora, Shimoshidami, Moriyama-ku, Nagoya, Aichi 463-8560, Japan

S Supporting Information

ABSTRACT: Seamless control of resistance to liquid drop movement for polar (water) and nonpolar alkane (*n*-hexadecane, *n*-dodecane, and *n*-decane) probe liquids on substrate surfaces was successfully demonstrated using molten linear poly(dimethylsiloxane) (PDMS) brush films with a range of different molecular weights (MWs). The ease of movement of liquid drops critically depended on polymer chain mobility as it relates to both polymer MW and solvent swelling on these chemically- and topographically identical surfaces. Our brush films therefore displayed lower resistances to liquid drop movement with decreasing polymer MW and surface tension of probe liquid as measured by contact angle (CA) hysteresis and tilt angle measurements. Subsequently, while mobility of water drops was inferior and became worse at higher MWs, *n*-decane drops were found to experience little resistance to movement on these polymer brush films. Calculating CA hysteresis as $\Delta\theta_{\cos} = \cos\theta_R - \cos\theta_A$ (θ_A and θ_R are the advancing and receding CAs, respectively) rather than the standard $\Delta\theta = \theta_A - \theta_R$ was found to be advantageous for estimation of the actual dynamic dewetting behavior of various probe liquids on an inclined substrate.



INTRODUCTION

Extensive research on the control of adhesion and dewetting of liquid drops from solid surfaces has been reported in the literature. Most studies related to this field have particularly focused on the effects of surface chemical makeup,^{1–10} chemical structure,^{4–6} and topography^{5,11–20} on the wetting/dewetting properties of the modified surface. Practically, the aim has been to produce functional surfaces with low resistance to gravity-driven movement on inclined surfaces. In this way, small-volume drops ($\sim 3\text{--}10\ \mu\text{L}$) can be easily set in motion to move across and off surfaces when the substrate tilt angle (TA) is low ($<10^\circ$). The lotus leaf surface is a good example from nature that demonstrates such excellent dynamic dewetting behavior with water.^{21–24} On the other end of the spectrum are adhesive/sticky surfaces on which liquid drops are pinned to the surface regardless of the magnitude of the static contact angle (CA, θ_S) and TA.²⁰ The typical hydrophobic glass window or car windshield, even after treatment with conventional perfluoroalkylsilanes, exhibits such inferior dynamic dewettability as is obvious on rainy days.

To accurately characterize the dewetting properties of a substrate surface, the measurement of dynamic (advancing (θ_A) and receding (θ_R)) CAs and the CA hysteresis are required.^{1–18,25–27} CA hysteresis is the mass-independent measure of the resistance to macroscopic liquid drop movement on inclined surfaces. It recognizes that, in order for the gravitational force to cause a liquid drop to depin from a stationary position on a horizontal surface and begin sliding/rolling down an inclined surface, the shape of the liquid drop first undergoes a certain amount of deformation (Figure 1).

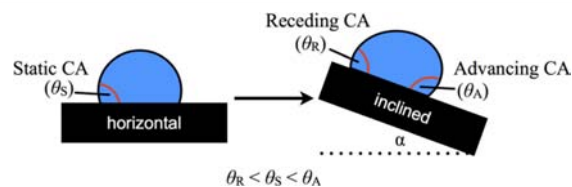


Figure 1. Comparison of liquid drops on horizontal and inclined surfaces.

This deformation from a section of a sphere results in an increase in the liquid–vapor interfacial area of the drop, assuming that the solid–liquid contact area remains constant or experiences a relatively insignificant change. The energy associated with this increase in liquid–vapor interfacial area has also been described as the activation energy barrier to liquid drop motion down an inclined substrate.^{16,17} From the initial horizontal position with θ_S , the drop begins movement when its contact lines at the front and back ends are capable of advancing and receding, respectively (Figure 1). These advancing and receding events occur at θ_A and θ_R , also the maximum and minimum possible CAs for a liquid–surface pair, respectively. CA hysteresis can be described by taking θ_A and θ_R into account as follows:

$$\Delta\theta_{\cos} = \cos\theta_R - \cos\theta_A \quad (1)$$

Equation 2 describes the gravitational force required to initiate drop movement across a tilted solid surface as being dependent

Received: March 25, 2012

Published: May 30, 2012

on $\Delta\theta_{\cos}$, where m is the mass of the drop, g is the gravitational constant, α is the TA, k is a constant that depends on drop shape, w is the width of the drop, and γ_{lv} is the liquid–vapor surface tension.^{5,9,27,28}

$$F = mg(\sin \alpha) = kw\gamma_{lv}(\cos \theta_R - \cos \theta_A) \quad (2)$$

When CA hysteresis is small enough, liquid drops then require low substrate TAs to depin from the horizontal position and begin moving down the surface without substantial drop shape deformation. Conversely, drops can remain permanently pinned to vertically oriented surfaces regardless of the magnitude of θ_S , if the CA hysteresis is significant.^{5,6,10,20,21} Previous publications have used a simpler definition of CA hysteresis ($\Delta\theta$)^{1,3,5–8,10–12,17,26} with no relation to the resulting minimum TA of a liquid drop on a surface:

$$\Delta\theta = \theta_A - \theta_R \quad (3)$$

The hydrophobic/oleophobic treatments of solid surfaces using ultrathin (<3 nm) smooth organic monolayers have been widely demonstrated and it is well-known that their surface chemistry^{1–3} and physical nature (solidlike or liquidlike)^{4–6} have a direct influence upon the CA hysteresis. Conventional self-assembled monolayers (SAMs) with high packing densities generally exhibit solidlike surface properties, resulting in sizable CA hysteresis.^{1–3} Simple reduction of packing density either through shortening the reaction time or use of specific chemical structures produces liquidlike surfaces with lower $\Delta\theta$.^{1,4–6} These actions are mainly aimed at increasing the physical mobility of the surface-tethered molecules to increase their responsiveness to the shearing force²⁶ from the moving contact line of the liquid drop. For example, a trimethylsilyl-terminated monolayer synthesized to possess the maximum achievable packing density through a 72 h vapor phase reaction exhibited $\theta_A/\theta_R = 105^\circ/96^\circ$ and $\Delta\theta = 9^\circ$.¹ However, by shortening the reaction time to 2.5 h, a chemically identical monolayer with lower packing densities and greater rotational freedom of the functional moieties was produced. The resulting $\Delta\theta$ was reduced from 9° to 3° ($\theta_A/\theta_R = 100^\circ/97^\circ$).¹ A subsequent investigation of the various types of trimethylsilyl-terminated organosilanes found that a highly mobile, branch-structured tris(trimethylsilyloxy)silylethylmethyl silane produced a surface with almost no $\Delta\theta$ ($\theta_A/\theta_R = 104^\circ/103^\circ$ and $\Delta\theta = 1^\circ$).^{4,16} On the basis of these fundamental studies, we have previously reported that extremely low $\Delta\theta$ surfaces for water and *n*-hexadecane could also be prepared using monolayers consisting of cyclic silanes⁵ and branch-structured perfluorinated silanes.⁶

In contrast to the research on the dewetting behavior of smooth monolayer surfaces, investigations into such properties of smooth polymer brush films have been limited to only static situations.^{29–52} Typically only θ_S of probe liquids at room temperature are reported to provide a qualitative measure of the chemistry of the polymer repeat unit.^{33–47} Even the CA data (for a variety of probe liquids) of bulk polymer surfaces listed in the *Polymer Data Handbook* only consists of θ_S values.⁵³ Dynamic CA measurements are scarce in reports describing the surface chemistry of smooth polymer brush films. Jordan et al. has reported θ_A and θ_R values of solidlike polystyrene (PS) brush films to be similar to that of solid bulk PS.²⁹ Minsky et al. also demonstrated that polymethylmethacrylate (PMMA)-PS random copolymer brushes exhibited increasing $\Delta\theta$ with increasing styrene fraction, but the reason has not yet been clearly explained.³⁰ The use of polymer brush films for the purpose of controlling the dynamic hydro-

phobicity/oleophobicity has been rarely seen. One recent publication has noted that $\Delta\theta$ was small for thin poly-(dimethylsiloxane) (PDMS) brush films consisting of very low MW polymer (MW 2000).⁷ However, the relationship between such polymer brush surfaces and the dynamic CA behavior for various probe liquids has not yet been clearly identified, particularly for molten polymer brush surfaces. If the resistance to polar and nonpolar liquid drop movement on inclined surfaces, as measured by CA hysteresis ($\Delta\theta$ or $\Delta\theta_{\cos}$) and minimum substrate TAs, could be controlled precisely, such a technique would make it very appealing for practical applications including microfluidics, micro/nanoelectromechanical systems, self-cleaning surfaces, and window coatings.

In this article, we report a comprehensive study with regard to tuning the dewettability of polymer brush films consisting of one homopolymer through the control of the physical polymer chain mobility. In doing so, we reveal a new approach that reduces the resistance to liquid drop movement with decreasing surface tension and carbon number of the alkane probe liquid on a surface that is smooth and nonperfluorinated. The dynamic dewetting behavior of liquid droplets was studied on linear PDMS^{53–55} brush films (Table 1) grafted to smooth Si

Table 1. PDMS Polymers Employed in This Study, and Their MW and Bulk Viscosity at 25 °C

PDMS MW	viscosity (cSt)
6000	100
17200	500
28000	1000
49500	5000
72000	20000
117000	60000

wafers. Linear PDMS serves as an ideal polymer, because it is highly molten at room temperature even at high MWs due to its extremely low glass transition temperature ($T_g = -127^\circ\text{C}$).^{53–55} As a liquid polymer melt, its chains naturally exhibit a finite chain mobility at room temperature. In comparison, many other polymers are solids with negligible chain mobility at ambient conditions, exhibiting T_g 's significantly higher than room temperature.^{53,54} PDMS has another advantage in that it is nonperfluorinated. Much of the recent focus of dewetting studies has been on the formation of perfluorinated rough surfaces.^{18,19} Such surfaces are effective in reducing interactions between the probe liquids (in particular, nonpolar liquids) and the surface since they force liquid drops to adopt the shape of balls with $\theta_S > 150^\circ$. However these surfaces usually exhibit increasing adhesion of the liquid drop to the surface from water to alkanes, as evidenced by the higher CA hysteresis and minimum TAs for the latter in comparison to the former. In addition, in order to prevent the alkane liquid from completely soaking into and wetting the roughened surface, perfluorinated surface chemistry is required. However with the recent concern for the chemical and physical effects of perfluorinated compounds on human health and the environment, development of nonperfluorinated surfaces showing excellent liquid dewetting properties is necessary.^{10,19,56,57} We have already made a preliminary report of the dynamic dewettability of a low MW (MW 6000) PDMS brush film surface, on which various probe liquids (polar and nonpolar, with high and low surface tensions) could move smoothly without pinning (excellent dynamic hydrophobicity/oleophobicity).¹⁰ We have therefore

extended our study to PDMS polymers with higher MWs (to MW 117000). They are still molten polymers and expected to form chemically identical surfaces. In this study, we have focused on the effects of polymer MW and solvent interactions on the dynamic dewetting behavior of various PDMS brush surfaces. These variables applied here are the most fundamental of factors with which to control molten polymer chain mobility and the resulting physically liquidlike nature of a low- T_g polymer brush film.^{10,54} Adjusting only these two simple physical parameters allowed for extremely fine control over the dynamic dewetting behavior of PDMS brush films toward various nonpolar alkane (*n*-hexadecane, *n*-dodecane, and *n*-decane) liquids. We further discuss the resistance to liquid drop movement of various probe liquids on inclined substrates using TAs and two different definitions of CA hysteresis ($\Delta\theta$ and $\Delta\theta_{\text{cos}}$). A shift in research focus from conventional static CAs (magnitude of CAs) to dynamic CAs and CA hysteresis exhibited by polar/nonpolar liquids on substrate surfaces is greatly needed for the design and preparation of potentially useful functional surfaces.

EXPERIMENTAL SECTION

Materials. 1,3,5,7-Tetramethylcyclotetrasiloxane (D_4^H), Karstedt's catalyst (2.1–2.4% Pt in xylene), and vinyl-terminated poly-

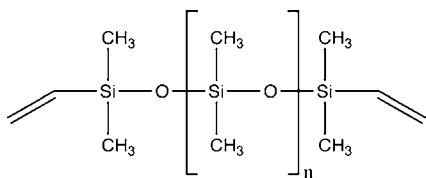


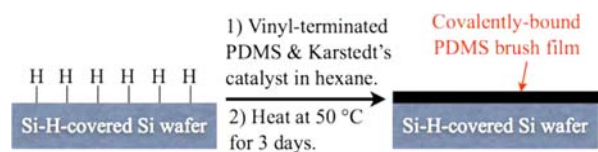
Figure 2. Vinyl-terminated PDMS.

(dimethylsiloxane) (PDMS) polymers (Figure 2) were purchased from Gelest Inc. (Morrisville, PA, USA) and used as received. Six different linear PDMS polymers were used in this study (Table 1).⁵⁵ *n*-Hexane (96+%, GC), *n*-decane (96+%, GC), *n*-dodecane (96+%, GC), *n*-hexadecane (96+%, GC), and acetone (99.5+%, GC) were purchased from Wako Inc. and used as received. Sample substrates ($10 \times 10 \times 0.5 \text{ mm}^3$) cut from *n*-type Si (100) wafers were photochemically cleaned by UV/ozone treatment.

Grafting PDMS Chains to Si Substrate. The cleaned, oxidized Si (Si^{SiO_2}) substrates were first exposed to D_4^H vapor in closed 60 cm^3 PFA block digestion vessels (Saville) in a N_2 atmosphere with less than 10% relative humidity for 3 days at 80 °C. Due to this vapor phase treatment, a D_4^H -monomeric layer (about 0.5 nm thick) was formed.^{6,10} Samples were rinsed with hexane, acetone, and water, in that order. The resulting surfaces exhibited dynamically hydrophobic and oleophobic properties (water: $\theta_A/\theta_R = 106^\circ/104^\circ$ and *n*-hexadecane: $33^\circ/31^\circ$, respectively) with low CA hysteresis ($\Delta\theta = 2^\circ$) for both probe liquids.^{6,10} The D_4^H -covered samples were then immediately placed in glass scintillation vials and submerged in hexane solutions consisting of 20 vol % vinyl-terminated PDMS and Karstedt's catalyst with concentration of 10 ppm Pt. Pt-catalyzed hydrosilylation^{10,58,59} was carried out for 3 days at 50 °C (Scheme 1). Samples were then rinsed with copious amounts of hexane, acetone, and water, in that order, to remove unreacted materials from the surface, leaving behind only PDMS chains tethered to the surface via ethylene linkages formed through Pt-catalyzed hydrosilylation.

Characterization. CA measurements were performed with a CA instrument (Kyowa Interface Science, CA-X). θ_S , θ_A and θ_R were collected using Milli-Q water ($10^{-18} \text{ } \Omega/\text{cm}$), *n*-hexadecane, *n*-dodecane, and *n*-decane at room temperature ($\sim 25 \text{ }^\circ\text{C}$). θ_S was measured by gently placing a drop of the probe liquid (3 μL) on the horizontal surface. θ_A and θ_R were measured as probe liquid (3 μL)

Scheme 1. Grafting of Vinyl-Terminated PDMS Chains to the Si–H (D_4^H -Monolayer)-Covered Si Wafer Surface



was added (θ_A) and withdrawn (θ_R) from the surface-bound drop. CAs were gathered at three different locations on each surface. θ_S , θ_A , and θ_R reported are the averages of the three values gathered. All values for each sample were in the range of $\pm 2^\circ$. Minimum substrate TAs necessary to initiate drop (3–10 μL) movement across surfaces were measured using a TA meter (Kyowa Interface Science) at three different locations on each surface. Film thicknesses were determined by ellipsometry (Philips, PZ2000) equipped with a He–Ne laser (632.8 nm) with its incident angle fixed at 70° . The topology of the samples was observed by atomic force microscopy (AFM, Seiko Instruments, SPA400) using a Si probe (SII, SI-DP20; spring constant = 15 N m^{-1}) with a response frequency of 135 kHz in the tapping mode.

RESULTS AND DISCUSSION

Formation and Characterization of the PDMS Brush Films. Six different vinyl-terminated linear PDMS polymers (Table 1) were tethered to the D_4^H -monolayer-covered Si^{SiO_2} surfaces through Pt-catalyzed hydrosilylation (Scheme 1). Consequently, as shown in Figure 3, chemically identical

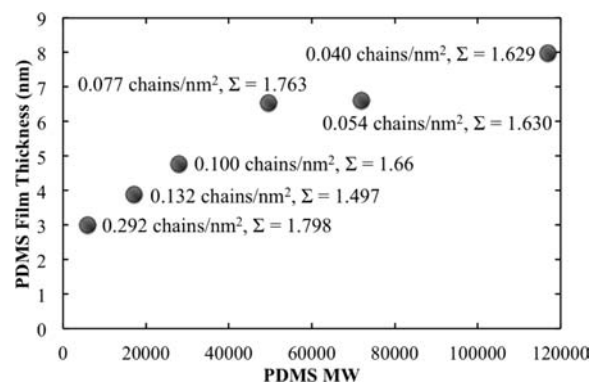


Figure 3. PDMS MW versus ellipsometrically estimated thickness and grafting density of the resulting PDMS brush film. Σ is the reduced tethering density.^{52,61}

PDMS brush films, with thicknesses ranging from 3 to 8 nm, were successfully produced. In a previous study, we confirmed that PDMS chains with MW 6000 were tethered to the D_4^H -covered Si^{SiO_2} surfaces through this reaction, such that the resulting PDMS brush film completely covered the surface.¹⁰ Here we found that the thicknesses of these brush films increased with MW and began to level off when the MW exceeded 49500 (PDMS MW 49500–117000). In addition, the thicknesses of our PDMS brush films were slightly larger ($\sim 8.7\%$ greater on average) than the diameter of the PDMS coil (twice the radius of gyration (R_g)). Therefore, the films can be viewed as a monomeric layer of coiled polymer chains. On the basis of this thickness data, the grafting densities of these chemically identical PDMS brush films were calculated to decrease from 0.292 to 0.040 chains/nm² with increasing MW (Figure 3), as expected in the polymer brush “grafting to” process.^{47,51,52} Such a trend has been frequently observed in the

grafting of other typical polymers such as poly(ethylene glycol) (PEG)⁴⁷ and polystyren⁵¹ to smooth polymer-coated Si^{SiO₂} surfaces. The reduced grafting density (Σ)^{52,61} of $1.50 < \Sigma < 1.80$ for all six PDMS brush films reflects this characterization. The films produced here are therefore considered to be in the “mushroom-to-brush-transition” regime. They are in great contrast with those produced by the “grafting from” process, for which polymer chains are highly stretched and packed in significantly higher grafting densities to be considered in the “brush” regime ($\Sigma > 5$).⁵²

In our present case, the vinyl moieties at the two ends of the linear PDMS chain are utilized to graft the PDMS chains to the reactive Si–H moieties on the D₄^H-covered Si^{SiO₂} surface (Scheme 1). In addition to CA measurements and ellipsometry, we also confirmed by infrared reflection absorption spectroscopy (IR-RAS) that Pt-catalyzed hydrosilylation was complete, since peaks of Si–H and vinyl groups are barely discernible, i.e. background level.¹⁰ However, the actual bonding situation, whether both ends or only one end of the PDMS chains is tethered to the surface, have not yet been identified, since their concentrations are extremely low (only 0.05–1.0 wt %).

The decrease in grafting density and increase in brush film thickness with increasing PDMS MW may be attributed to the reactive ends becoming kinetically trapped within the polymer coil and unable to reach the reactive sites on the surface.^{47,51,52} The possibility of these end groups buried within the PDMS coil, diffusing out and becoming accessible to the Si–H groups, decreases with increasing MW. In addition, the increase in MW of the PDMS chains also leads to greater R_g 's of the polymer coil grafted to the surface, which possibly blocks a wider area of Si–H surface groups and limits their ability to engage in hydrosilylation.

In spite of the increase in film thickness with higher MW, there were no marked differences in surface morphologies for all samples. As shown in a typical AFM image of the PDMS surface in Figure 4, the brush film (PDMS MW 28000)

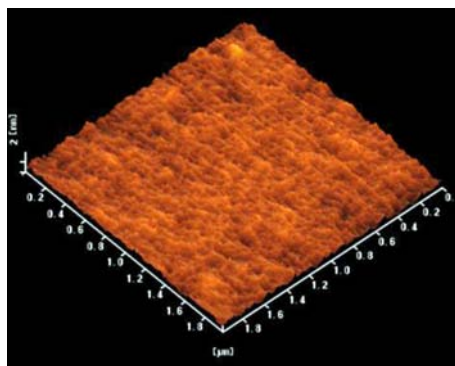


Figure 4. AFM image of a typical PDMS brush film ($2 \times 2 \mu\text{m}^2$) formed by the “grafting-to” process using Pt-catalyzed hydrosilylation (in this case, PDMS MW 28000).

homogeneously covered the Si^{SiO₂} surface and was extremely smooth with a root-mean-square roughness (R_{rms}) of 0.330 nm ($2 \times 2 \mu\text{m}^2$). No aggregates, defects, or additional topography were observed over the entire substrate. All PDMS film surfaces appeared to be similar to that of the cleaned Si^{SiO₂} substrate (R_{rms} of ~ 0.2 nm). AFM confirmed that, independent of the film thickness and grafting density, surface morphologies remained unchanged ($R_{\text{rms}} < 0.8$ nm) (Table 2). The smoothness and complete surface coverage of our PDMS

Table 2. Surface Roughness Data Estimated from AFM Images of the Six PDMS Brush Films ($2 \times 2 \mu\text{m}^2$)

PDMS MW	R_{rms} (nm)
6000	0.374
17200	0.337
28000	0.330
49500	0.751
72000	0.724
117000	0.737

brush films are in very good agreement with those previously reported by the authors¹⁰ and others.^{7,8} Furthermore, PDMS is one of the few linear polymers to be considered a liquid at room temperature even at extremely high MWs. Its T_g is very low at -127 °C, and it remains stable at temperatures over 200 °C.^{53,55} These results offer clear evidence that the chemistry and conditions employed in this study have no influence upon the PDMS repeat unit (the MW of the chains tethered to the surface remained unchanged from the bulk) and surface morphologies. In the absence of any chemical or topographical differences between the six PDMS brush films, the variations in their dewetting properties are therefore governed by differences in surface physical properties.

Effects of Polymer MW on the Dynamic Dewettability of PDMS Brush Films. As described in the previous section, our brush films showed complete surface coverage and were nearly identical both chemically and topographically. As a result of the decrease in probe liquid surface tension (Table 3), the

Table 3. Properties of the Probe Liquids Compared to Those of PDMS

probe liquid	surface tension (dyn/cm) ^a	solubility parameter (MPa) ^{1/2b}
water	72.8	47.8
<i>n</i> -hexadecane	27.5	16.3
<i>n</i> -dodecane	25.4	16.0
<i>n</i> -decane	23.8	15.7
PDMS	20.9–21.5 ^c	15.1 ^c

^aAt 20 °C (from ref 63). ^bFrom ref 64. ^cFrom ref 53.

liquid drop profile (Figure 5a) and the resulting θ_s values on the polymer brush surface decreased from water to *n*-decane. However, as clearly seen in Figure 5b, the θ_s values of water, *n*-hexadecane, *n*-dodecane, and *n*-decane were practically identical over the entire range of MWs. There was no apparent relationship between the θ_s values of four probe liquids and the MW of PDMS polymers. In contrast to such static situations, dynamic CA behavior toward all probe liquids on these surfaces showed strong correlation with MW. Figure 6a clearly indicates that CA hysteresis ($\Delta\theta_{\text{cos}} = \cos\theta_{\text{R}} - \cos\theta_{\text{A}}$) increased for the four probe liquids with an increase in MW. As shown in Figure 7, θ_{A} and θ_{R} values appeared to diverge approximately from the θ_s values for the respective probe liquids. This phenomenon can be understood by regarding the motion of the advancing and receding contact lines of the liquid drops acting as a shearing force on the surface-tethered polymer chains.²⁶ The ability of the mobile polymer chains to respond to such external forces is strongly dependent on the MW. Such MW-dependent physical chain mobilities exist in both three-dimensional (3-D) bulk polymer melts and two-dimensional (2-D) polymer brush films.^{66,67} Therefore, at low MW, the high chain mobility allows the surface to exhibit significant liquidlike behavior. The shorter

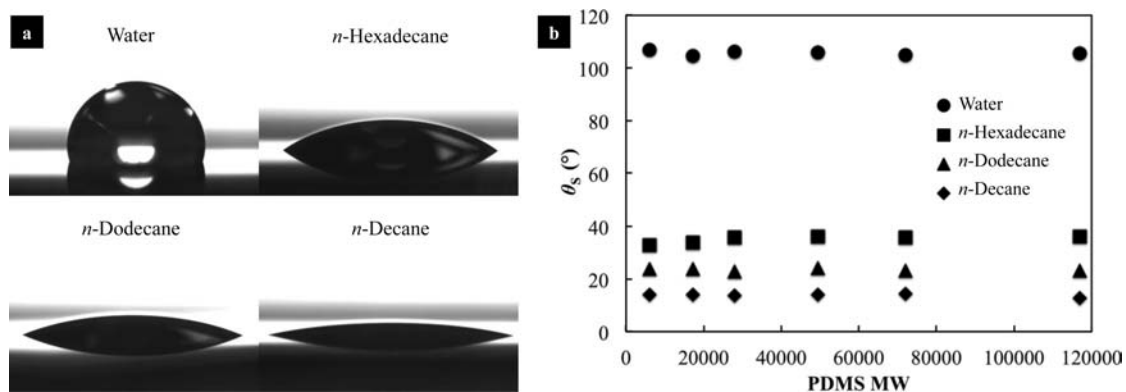


Figure 5. (a) Pictures of 3 μL -sized liquid drops on the PDMS brush surface and (b) static CAs versus PDMS MW for the four probe liquids.

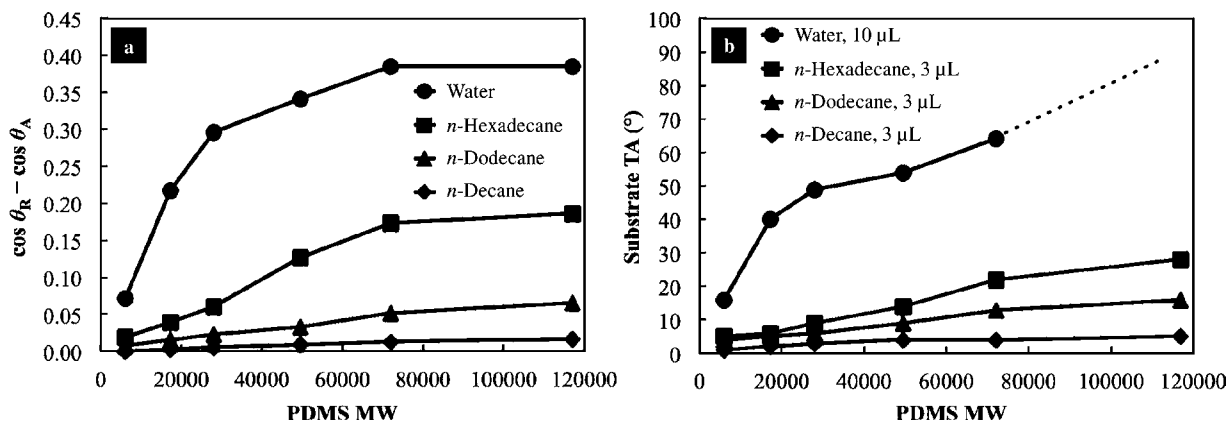


Figure 6. (a) Changes in CA hysteresis of the grafted PDMS brush surfaces with MW for water, *n*-hexadecane, *n*-dodecane, and *n*-decane. (b) Changes in minimum substrate TAs of the grafted PDMS brush surfaces with MW for water, *n*-hexadecane, *n*-dodecane, and *n*-decane. For water at MW 117000, the droplet remained pinned at TA of 90°.

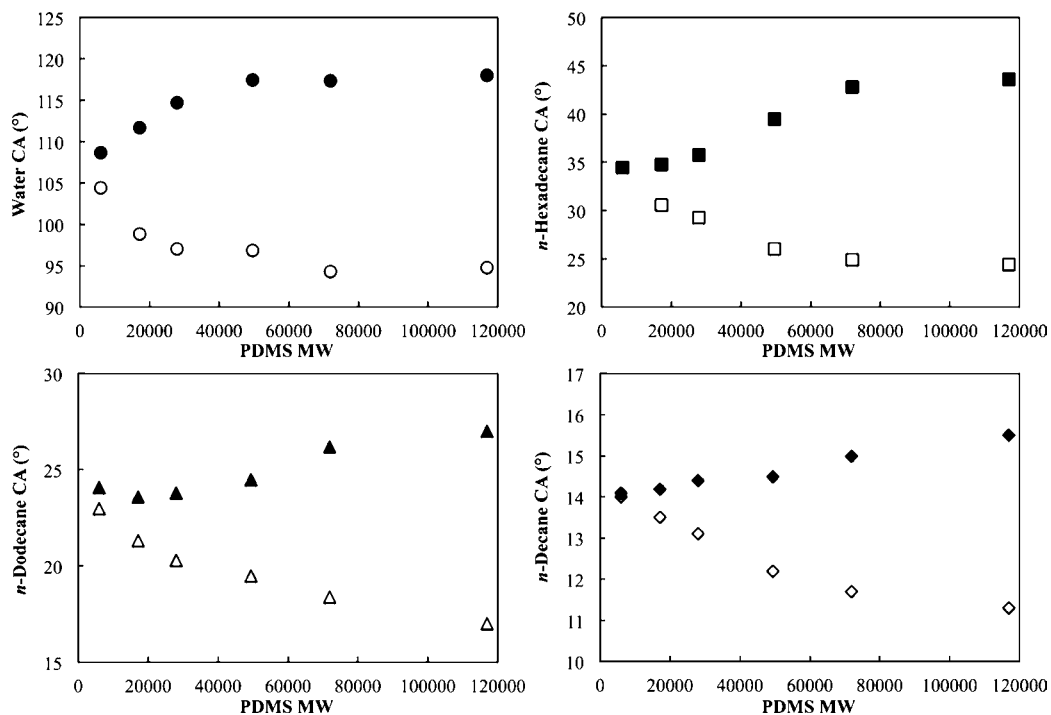


Figure 7. Changes in θ_A (closed symbols) and θ_R (open symbols) with MW of the grafted PDMS brush surfaces for water, *n*-hexadecane, *n*-dodecane, and *n*-decane.

polymer chains provide less resistance to the motion of the advancing and receding contact lines of the probe liquids, resulting in lower CA hysteresis. On the other hand, higher MWs impart a more solidlike character to the surface. The longer chain lengths cause the mobility of the chains to become increasingly sluggish. This leads to greater resistance to contact line motion, resulting in greater CA hysteresis. These radical differences in chain mobility are evident by the significant variations in PDMS bulk viscosity with MW. PDMS with MW 117000 has a MW 19.5 times greater than that of PDMS with MW 6000, but its viscosity, resembling very thick honey, is 600 times that of the latter which has the liquid consistency of vegetable oil (Table 1). The dependence of such resistance on the physical nature of the polymer brush films is corroborated by θ_A , θ_R , and CA hysteresis of the four probe liquids extrapolating accurately to those of bulk cross-linked Sylgard 184.⁶⁸ This silicone elastomer can be considered to be solid PDMS with infinite MW and viscosity, possessing negligible chain mobility. θ_A and θ_R values of water, *n*-hexadecane, *n*-dodecane and *n*-decane on this surface were 122°/96°, 44°/23°, 28°/16°, and 18°/10°, respectively, in order of decreasing surface tension. Similarly, CA hysteresis ($\Delta\theta_{\text{cos}}$) was 0.425, 0.201, 0.078, and 0.025, respectively. These values are nearly identical to those observed in the brush surfaces prepared with higher MWs of PDMS (Figure 6a). Thus, we can conclude that such surfaces show solidlike properties. In addition to this, Krumpfer et al. suggested that the “lenses” that probe liquid drops form on thicker films of liquid silicones (in their case, >12 nm) contribute to CA hysteresis.⁸ Such an effect is also responsible to a certain extent for the large CA hysteresis observed on our thick brush surfaces prepared by PDMS MWs of 49500, 72000, and 117000. This increase in resistance to liquid drop movement with PDMS MW was confirmed by the increase in TAs required to set microliter-sized drops of the four probe liquids into motion (Figure 6b). Our assumption was further supported by a subsequent set of experiments. The PDMS brush film surfaces prepared through the direct grafting method reported by Krumpfer et al.^{7,8} with the PDMS polymers used here exhibited nearly identical dynamic CA behavior over the entire MW range of PDMS (see Supporting Information, Figures S-1 and S-2).⁶⁹ Although these PDMS brush films had different polymer chain end-group chemistry, brush film thicknesses, and grafting densities, dynamic CAs and CA hysteresis were in good agreement with our data. This clearly demonstrates that dynamic CA behavior markedly depends on physical chain mobility with varying PDMS MW.

Solvent Effects of Probe Liquids on the Dynamic Dewettability. Besides the effects of polymer MW on the chain mobilities of our PDMS brush films, the affinity between the probe liquids and polymer chains is another physical variable available for controlling the chain mobility. Generally, the chemistry of polymer brush films allows it to interact with and be swollen by liquids that are classified as good solvents for that polymer.^{48–50,62} As shown in Figure 6a, the CA hysteresis for alkane liquids was significantly lower than that for water. This is due to the increase in chain mobility resulting from the swelling of the PDMS brush films by alkane liquids. For example, as previously reported by the authors, the excellent solubility of PDMS 6000 in *n*-hexadecane produced a “blended liquid–liquid interface” between the probe liquid and the PDMS MW 6000 brush film surface.¹⁰ This solubility of PDMS with MW 6000 with *n*-hexadecane resulted in the enhancement of the liquidlike property of the brush films. The interface is

characterized by the extended conformations of the surface-tethered polymer chains into the probe liquid drop due to their solvent-swollen state. In contrast, water is a nonsolvent for PDMS and produced a “discrete liquid–liquid interface”, similar to that between bulk oil and water phases. The chain conformations of the PDMS coils are collapsed in comparison to the solvent-swollen state, resulting in lower chain mobility. Therefore, CA hysteresis of *n*-hexadecane was considerably lower than that of water. In addition, the magnitude of CA hysteresis was markedly influenced by the degree of swelling of our PDMS brush films by the probe liquids. The decreasing difference between the solubility parameter ($\Delta\delta$) of PDMS and the probe liquid from *n*-hexadecane to *n*-decane illustrates that the lower carbon number alkanes are capable of greater solvent interactions than those with higher carbon alkanes (Table 3). Thus the extent of swelling of the PDMS brush films by the probe liquid increases accordingly. However, as shown in Figures 5–7, despite the solvent interactions at the “blended liquid–liquid interfaces”, the alkane liquids used here are still capable of forming a CA on PDMS without completely wetting and soaking into the surface ($\theta_A/\theta_R = 0^\circ/0^\circ$).⁶⁵

According to the pictures of the four probe liquids shown in Figure 5a, the PDMS brush surface can be considered to be statically oleophilic but fairly hydrophobic. However, as mentioned before, the CA hysteresis of water was considerably larger than those of the alkane liquids, increasing from 0.22 to 0.38 with MW (Figure 6a). Therefore minimum substrate TA was large even for 10 μL water drops, starting at 16° at MW 6000 and becoming permanently pinned on the vertically oriented PDMS brush surface with MW 117000 (Figure 6b). Conversely, for the alkane probe liquids at all PDMS MWs, CA hysteresis and minimum substrate TAs for only 3 μL drops were considerably lower than those for water, and also decreased with lower carbon number and surface tension of alkane liquid. With increasing MW, CA hysteresis described by eq 1 ranged from 0.019 to 0.187 (*n*-hexadecane), from 0.008 to 0.065 (*n*-dodecane), and from 0.0004 to 0.017 (*n*-decane). Minimum substrate TAs for 3 μL -sized alkane drops therefore correspondingly decreased with carbon number while still increasing with MW. Moreover, in the case of the PDMS brush film with MW 6000, only 1° of substrate incline was sufficient to initiate movement for a 3 μL drop of *n*-decane (Movie S-1, see Supporting Information). This value is over 5 times smaller than that reportedly needed for a larger *n*-decane drop (5 μL) on a superoleophobic surface with $\theta_s > 160^\circ$.¹⁹ The significant reductions in resistance to liquid drop movement are due to the extended chain conformations of PDMS chains with alkanes compared to the collapsed conformations with water. The extended conformations of solvent-swollen chains then produced greater polymer chain mobility, as mentioned before. Solvent swelling also increased from *n*-hexadecane to *n*-decane, thereby further increasing chain mobility. Importantly, these improvements in liquid dewettability from polymer brush films occurred with increases in the contact area between the liquid drop and the PDMS surface and decreases in the profile of the drop shape. Our results demonstrated here mark a complete reversal of research outcomes of superhydrophobic/superoleophobic studies which just focused on increasing static CAs and decreasing the contact area between the liquid drop and surface.

Unusual Insight into Resistances against Solid Matter and Liquid Movement on Polymer Brush Surfaces. The results of this study highlight a significant analogous relation-

ship between the resistances against movement of liquid and solid matter over polymer brush films, as measured by CA hysteresis and the coefficient of friction,^{49,67,70,71} respectively. For polymer brush films, the movement of solid matter across such brush films have also been viewed as shearing forces on the surface-tethered polymer chains.⁶⁷ From this viewpoint, studies have connected the same fundamental tenets of polymer physics covering polymer chain mobility applied here, to the lubricating behavior and subsequent friction coefficient of molten and solvent-swollen polymer brush films. Klein et al.⁷⁰ first pointed out that surface-tethered polymer chains exhibited a striking reduction in friction coefficient when swollen by a solvent. The extended conformation of the solvent-swollen polymer chains produced greatly improved lubricating properties. Friction coefficients of polymer brush films have also been shown to be solvent dependent. Due to the greater interactions between polymer chains and a good solvent, the resulting friction coefficient was 3 orders of magnitude lower than that of the polymer brush in a poor solvent environment.⁷¹ Landherr et al.⁶⁷ later reported that friction coefficients of PDMS brush films also decreased with MW, despite the identical chemical makeup of the surfaces. Increasing MW from 10000 to 52000 resulted in a comparable increase in friction coefficient. This was the result of shorter relaxation times and lower film viscosities of brushes composed of lower MW polymer. Indeed, these reports showed that adjusting the physical nature of the surfaces alone also generated significant differences in the resistance against movement of solids across those surfaces. With such important parallels between these two areas of research emerging from the results presented here, this study clearly re-emphasizes that CA hysteresis, not static CAs and the shape of the drop, is a critical necessity for accurately representing and understanding the resistance to depinning and dewetting of liquid drops from solid surfaces.

Comparing Definitions of CA Hysteresis. Finally, we discuss the dynamic dewetting behavior of the four probe liquids using the two different definitions of CA hysteresis described in eqs 1 and 3. In comparison to the conventional definition of CA hysteresis ($\Delta\theta$), the use of the alternative definition of CA hysteresis ($\Delta\theta_{\cos}$) in this study is very advantageous, because the latter takes into account the magnitude of the actual CAs. This then demonstrates that, for example, a drop on a surface with $\theta_A/\theta_R = 100^\circ/90^\circ$ ($\Delta\theta_{\cos} = 0.174$) will be correctly described as having greater resistance to liquid drop movement than on a surface with $\theta_A/\theta_R = 50^\circ/40^\circ$ ($\Delta\theta_{\cos} = 0.123$), despite the same 10° difference. Therefore, the overall plot of CA hysteresis for the four probe liquids using $\Delta\theta_{\cos}$ in Figure 6a more closely resembles that of the minimum substrate TAs in Figure 6b. Both $\Delta\theta_{\cos}$ and TA curves for water are clearly separate and at much larger values than those of the alkane liquids which are grouped together. This points to the enormous advantageous influence of polymer brush swelling on the dewetting behavior of polymer brush films. In comparison, the use of the simpler definition of CA hysteresis clearly demonstrates a significant lack of connectivity between the $\Delta\theta$ values and the TAs, as shown in Figure 8. The $\Delta\theta$ curves for each of the four liquids with increasing MW are more equally separated from each other with significantly less correlation with the TA curves.

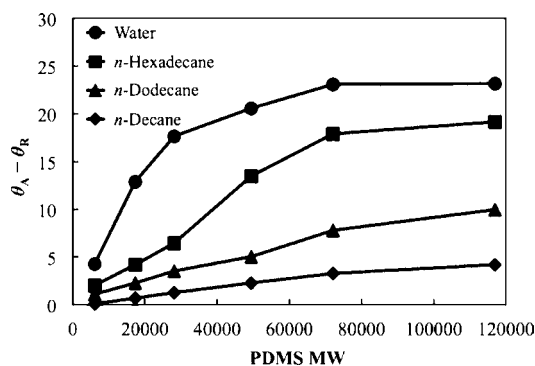


Figure 8. Changes in $\Delta\theta$ of the grafted PDMS brush surfaces with MW for water, *n*-hexadecane, *n*-dodecane, and *n*-decane.

CONCLUSIONS

We have successfully demonstrated that the dynamic dewetting behavior of water and alkane liquids could be finely tuned through physical control of the polymer chain mobility in PDMS brush films. Specifically, such command was effectively carried out through polymer MW and solvent effects by the probe liquids. Our principle described here is simple and effective, yet may provide highly effective and practical results by exploiting inherent physical properties of other molten and/or solvent-swollen polymer brush systems to tune resistance to the motion of the liquid drop contact line and subsequent ease of liquid drop movement. By taking a thermodynamically favorable approach that is the opposite of the forceful methods of conventional superhydrophobic/superoleophobic studies, we show that extremely low resistance to liquid drop movement can be effortlessly achieved by increasing interactions between the probe liquid and surface-tethered polymer chains. In fact, generating easy movement on inclined surfaces for drops of any liquid can be as simple as specifically grafting a polymer brush to the surface such that the liquid can swell the polymer chains without completely soaking into and wetting the film. We emphasize that control over the actual ease of gravity-driven motion of polar and nonpolar droplets down-tilted surfaces is more practically important than the maximum achievable static CA and minimum contact area between the probe liquid and the surface. We believe our principle provides a new understanding for fundamental studies on surface chemistry and the industrial applications thereof.

ASSOCIATED CONTENT

Supporting Information

Comparison of contact angles, contact angle hysteresis, and thicknesses for PDMS brush films prepared by a second method. This material is available free of charge via the Internet at <http://pubs.acs.org>.

AUTHOR INFORMATION

Corresponding Author

a.hozumi@aist.go.jp

Notes

The authors declare no competing financial interest.

ACKNOWLEDGMENTS

A. H., D. F. C., and C. U. express thanks to the City Area Program (development state) southern Gifu Area Development of Advanced Medical Equipments by Utilizing Manufacturing

Information Technologies and a Grand-in Aid for Scientific Research (23850020) of Ministry of Education, Culture, Sports, Science and Technologies (MEXT) for partial support. The authors also express gratitude to Dr. Makoto Yagihashi of Nagoya Municipal Industrial Research Institute for his technical assistance.

REFERENCES

- (1) Fadeev, A. Y.; McCarthy, T. J. *Langmuir* **1999**, *15*, 3759–3766.
- (2) Fadeev, A. Y.; McCarthy, T. J. *Langmuir* **2000**, *16*, 7268–7274.
- (3) Extrand, C. W. *Langmuir* **2003**, *19*, 3793–3796.
- (4) Fadeev, A. Y.; McCarthy, T. J. *Langmuir* **1999**, *15*, 7238–7243.
- (5) Hozumi, A.; McCarthy, T. J. *Langmuir* **2010**, *26*, 2567–2573.
- (6) Hozumi, A.; Cheng, D. F.; Yagihashi, M. J. *Colloid Interface Sci.* **2011**, *353*, 582–587.
- (7) Krumpfer, J. W.; McCarthy, T. J. *Faraday Discuss.* **2010**, *146*, 103–111.
- (8) Krumpfer, J. W.; McCarthy, T. J. *Langmuir* **2011**, *27*, 11514–11519.
- (9) Wier, K. A.; Gao, L. C.; McCarthy, T. J. *Langmuir* **2006**, *22*, 4914–4916.
- (10) Cheng, D. F.; Urata, C.; Yagihashi, M.; Hozumi, A. *Angew. Chem., Int. Ed.* **2012**, *51*, 2956–2959.
- (11) Chen, W.; Fadeev, A. Y.; Hsieh, M. C.; Oner, D.; Youngblood, J.; McCarthy, T. J. *Langmuir* **1999**, *15*, 3395–3399.
- (12) Oner, D.; McCarthy, T. J. *Langmuir* **2000**, *16*, 7777–7782.
- (13) Gao, L. C.; McCarthy, T. J. *Langmuir* **2006**, *22*, 2966–2967.
- (14) Gao, L. C.; McCarthy, T. J. *Langmuir* **2006**, *22*, 5998–6000.
- (15) Gao, L. C.; McCarthy, T. J. *J. Am. Chem. Soc.* **2006**, *128*, 9052–9053.
- (16) Gao, L. C.; McCarthy, T. J. *Langmuir* **2006**, *22*, 6234–6237.
- (17) Gao, L. C.; McCarthy, T. J. *Langmuir* **2009**, *25*, 14105–14115.
- (18) Tuteja, A.; Choi, W.; Ma, M. L.; Mabry, J. M.; Mazzella, S. A.; Rutledge, G. C.; McKinley, G. H.; Cohen, R. E. *Science* **2007**, *318*, 1618–1622.
- (19) Zhang, J. P.; Seeger, S. *Angew. Chem., Int. Ed.* **2011**, *50*, 6652–6656.
- (20) Jin, M. H.; Feng, X. J.; Feng, L.; Sun, T. L.; Zhai, J.; Li, T. J.; Jiang, L. *Adv. Mater.* **2005**, *17*, 1977–1981.
- (21) Deng, X.; Mammen, L.; Hans-Jürgen, B.; Vollmer, D. *Science* **2012**, *335*, 67–70.
- (22) Wangner, P.; Fürstner, R.; Barthlott, W.; Neinhuis, C. *J. Exp. Bot.* **2003**, *54*, 1295–1303.
- (23) Barthlott, W.; Neinhuis, C. *Planta* **1997**, *202*, 1–8.
- (24) Neinhuis, C.; Barthlott, W. *Ann. Bot.* **1997**, *79*, 667–677.
- (25) Koch, K.; Neinhuis, C.; Ensikat, H.-J.; Barthlott, W. *J. Exp. Bot.* **2004**, *55*, 711–718.
- (26) Gao, L. C.; McCarthy, T. J. *Langmuir* **2008**, *24*, 9183–9188.
- (27) Kawasaki, K. J. *Colloid Sci.* **1960**, *15*, 402–407.
- (28) Furmidge, C. G. J. *Colloid Sci.* **1962**, *17*, 309–324.
- (29) Jordan, R.; Ulman, A.; Kang, J. F.; Rafailovich, M. H.; Sokolov, J. *J. Am. Chem. Soc.* **1999**, *121*, 1016–1022.
- (30) Mansky, P.; Liu, Y.; Huang, E.; Russell, T. P.; Hawker, C. J. *Science* **1997**, *275*, 1458–1460.
- (31) Milner, S. T.; Witten, T. A.; Cates, M. E. *Macromolecules* **1988**, *21*, 2610–2619.
- (32) Auroy, P.; Auvray, L.; Leger, L. *Phys. Rev. Lett.* **1991**, *66*, 719–722.
- (33) Luzinov, I.; Minko, S.; Tsukruk, V. V. *Prog. Polym. Sci.* **2004**, *29*, 635–698.
- (34) Sidorenko, A.; Minko, S.; Schenk-Meuser, K.; Duschner, H.; Stamm, M. *Langmuir* **1999**, *15*, 8349–8355.
- (35) Motornov, M.; Minko, S.; Eichhorn, K. J.; Nitschke, M.; Simon, F.; Stamm, M. *Langmuir* **2003**, *19*, 8077–8085.
- (36) Yoshikawa, C.; Goto, A.; Tsujii, Y.; Fukuda, T.; Yamamoto, K.; Kishida, A. *Macromolecules* **2005**, *38*, 4604–4610.
- (37) Minko, S.; Muller, M.; Motornov, M.; Nitschke, M.; Grundke, K.; Stamm, M. *J. Am. Chem. Soc.* **2003**, *125*, 3896–3900.
- (38) Feng, X.; Zhai, J.; Jiang, L. *Angew. Chem., Int. Ed.* **2005**, *44*, 5115–5118.
- (39) Lim, H. S.; Lee, W. H.; Lee, S. G.; Lee, D.; Jeon, S.; Cho, K. *Chem. Commun.* **2010**, *46*, 4336–4338.
- (40) Wang, R.; Hashimoto, K.; Fujishima, A.; Chikuni, M.; Kojima, E.; Kitamura, A.; Shimohigoshi, M.; Watanabe, T. *Nature* **1997**, *388*, 431–432.
- (41) Lahann, J.; Mitragotri, S.; Tran, T. N.; Kaido, H.; Sundaram, J.; Choi, I. S.; Hoffer, S.; Somorjai, G. A.; Langer, R. *Science* **2003**, *299*, 371–374.
- (42) Kakade, B.; Mehta, R.; Durge, A.; Kulkarni, S.; Pillai, V. *Nano Lett.* **2008**, *8*, 2693–2696.
- (43) Tian, D.; Chen, Q.; Nie, F.; Xu, J.; Song, Y.; Jiang, L. *Adv. Mater.* **2009**, *21*, 3744–3749.
- (44) Xia, H. W.; Xia, F.; Tang, Y. C.; Guo, W.; Hou, X.; Chen, L.; Hou, Y.; Zhang, G. Z.; Jiang, L. *Soft Matter* **2011**, *7*, 1638–1640.
- (45) Sun, T. L.; Wang, G. J.; Feng, L.; Liu, B. Q.; Ma, Y. M.; Jiang, L.; Zhu, D. B. *Angew. Chem., Int. Ed.* **2004**, *43*, 357–360.
- (46) Sun, T. L.; Wang, G. J.; Feng, L.; Liu, B. Q.; Ma, Y. M.; Jiang, L.; Zhu, D. B. *Angew. Chem., Int. Ed.* **2004**, *43*, 357–360.
- (47) Zdyrko, B.; Varshney, S. K.; Luzinov, I. *Langmuir* **2004**, *20*, 6727–6735.
- (48) Huang, H.; Chung, J. Y.; Nolte, A. J.; Stafford, C. M. *Chem. Mater.* **2007**, *19*, 6555–6560.
- (49) Raviv, U.; Glasson, S.; Kamph, N.; Gohy, J. F.; Jérôme, R.; Klein, J. *Nature* **2003**, *425*, 163–165.
- (50) Advincola, R. C.; Brittain, W. J.; Caster, K. C.; Rühle, J. *Polymer Brushes*; Wiley-VCH Verlag GmbH & Co. KGaA: Weinheim, 2004.
- (51) Iyer, K. S.; Zdyrko, B.; Malz, H.; Pionteck, J.; Luzinov, I. *Macromolecules* **2003**, *36*, 6519–6526.
- (52) Brittain, W. J.; Minko, S. J. *Polym. Sci., Polym. Chem.* **2007**, *45*, 3505–3512.
- (53) Mark, J. E. *Polymer Data Handbook*; Oxford University Press Inc.: New York, 1999; pp 411–435.
- (54) Sperling, L. H. *Introduction to Physical Polymer Science*, 4th ed.; John Wiley & Sons Inc.: NJ, 2006.
- (55) Arkles, B.; G. Larson. *Silicon Compounds: Silanes & Silicones*; Gelest, Inc.: Morrisville, PA, 2008, pp 462–487.
- (56) Zushi, Y.; Hogarth, J. N.; Masunaga, S. *Clean Technol. Environ. Policy* **2012**, *14*, 9–20.
- (57) Lindstrom, A. B.; Strynar, M. J.; Libelo, E. L. *Environ. Sci. Technol.* **2011**, *45*, 7954–7961.
- (58) Surface tensions were obtained from the Landolt–Börnstein Database.
- (59) Stein, J.; Lewis, L. N.; Gao, Y.; Scott, R. A. *J. Am. Chem. Soc.* **1999**, *121*, 3693–3703.
- (60) Zheng, P. W.; McCarthy, T. J. *Langmuir* **2010**, *26*, 18585–18590.
- (61) $\Sigma = \sigma R_g^2$, where R_g is radius of gyration of a tethered chain at specific experimental conditions of solvent and temperature. The definition of grafting density (σ) is determined by $\sigma = (h\rho N_A)/M_n$ (h , brush thickness; ρ , bulk density of the brush composition; N_A , Avogadro's number; M_n , number-averaged MW).
- (62) We confirmed the solubility of PDMS in *n*-hexadecane, *n*-dodecane, and *n*-decane, and easily prepared 10 wt% PDMS solutions for all but PDMS MW 72000 and 117000 in *n*-hexadecane. PDMS MW 72000 and 117000 brush films likely remained moderately plasticized in *n*-hexadecane because of the only 1.2 MPa^{1/2} difference between their solubility parameters.
- (63) Surface tensions were obtained from the Landolt–Börnstein Database.
- (64) Hansen, C. M. *Hansen Solubility Parameters: A User's Handbook*; CRC Press: Boca Raton FL, 2007.
- (65) Stuart, M. A. C.; de Vos, W. M.; Leermakers, F. A. M. *Langmuir* **2006**, *22*, 1722–1728.
- (66) Luap, C.; Goedel, W. A. *Macromolecules* **2001**, *34*, 1343–1351.
- (67) Landherr, L. J. T.; Cohen, C.; Agarwal, P.; Archer, L. A. *Langmuir* **2011**, *27*, 9387–9395.

(68) Sylgard 184 Elastomer KIT (Dow Corning) was used. A slab of Sylgard 184 elastomer was produced using a 10:1 w/w of the base and curing agent, respectively. The two components were manually mixed vigorously for 5 min and then poured into a poly(ethylene terephthalate) tray $2.7 \times 2.7 \times 0.5 \text{ cm}^3$. It was allowed to cure at room temperature for 24 h, then cured for another 24 h at $80 \text{ }^\circ\text{C}$. Finally, the solid smooth elastomer was peeled out of the tray.

(69) The chemistry utilized by Krumpfer and McCarthy (refs 7 and 8) involved cleavage of the Si-O bond in the backbone of the PDMS polymer by surface charged species. Through this method, the resulting MW of the polymers chains in the resulting PDMS brush films was not the same as that of the original bulk polymer.

(70) Klein, J.; Kumacheva, E.; Mahalu, D.; Perahia, D.; Fetters, L. J. *Nature* **1994**, *370*, 634–636.

(71) Limpoco, F. T.; Advincula, R. C.; Perry, S. S. *Langmuir* **2007**, *23*, 12196–12201.